RESEARCH ARTICLE

WILEY

Reconstructed human skin shows epidermal invagination towards integrated neopapillae indicating early hair follicle formation in vitro

Irit Vahav[1,2] | Lenie J. van den Broek[2,3] | Maria Thon[2] | Hanneke N. Monsuur[2] | Sander W. Spiekstra[2] | Beren Atac[1,4] | Rik J. Scheper[3] | Roland Lauster[4] | Gerd Lindner[1,4] | Uwe Marx[1] | Susan Gibbs[2,5] [ID]

[1]TissUse GmbH, Berlin, Germany

[2]Department of Molecular Cell Biology and Immunology, Amsterdam Movement Sciences, VU University Medical Centre, Amsterdam UMC, Amsterdam, The Netherlands

[3]A-Skin BV, Amsterdam, The Netherlands

[4]Department of Biotechnology, Technische Universität Berlin, Berlin, Germany

[5]Department of Oral Cell Biology, Academic Centre for Dentistry Amsterdam (ACTA), University of Amsterdam and Vrije Universiteit Amsterdam, Amsterdam, The Netherlands

Correspondence
Susan Gibbs, Department of Molecular Cell Biology and Immunology, Amsterdam Movement Sciences, VU University Medical Centre, Amsterdam UMC, Amsterdam, The Netherlands.
Email: s.gibbs@vumc.nl

Abstract

Application of reconstructed human Skin (RhS) is a promising approach for the treatment of extensive wounds and for drug efficacy and safety testing. However, incorporating appendages, such as hair follicles, into RhS still remains a challenge. The hair follicle plays a critical role in thermal regulation, dispersion of sweat and sebum, sensory and tactile functions, skin regeneration, and repigmentation. The aim of this study was to determine whether human neopapilla could be incorporated into RhS (differentiated epidermis on fibroblast and endothelial cell populated dermis) and whether the neopapillae maintain their inductive follicular properties in vitro. Neopapillae spheroids, constructed from expanded and self-aggregating dermal papilla cells, synthesized extracellular matrix typically found in follicular papillae. Compared with dermal fibroblasts, neopapillae showed increased expression of multiple genes (Wnt5a, Wnt10b, and LEF1) known to regulate hair development and also increased secretion of CXCL1, which is a strong keratinocyte chemoattractant. When neopapillae were incorporated into the dermis of RhS, they stimulated epidermal down-growth resulting in engulfment of the neopapillae sphere. Similar to the native hair follicle, the differentiated invaginating epidermis inner side was keratin 10 positive and the undifferentiated outer side keratin 10 negative. The outer side was keratin 15 positive confirming the undifferentiated nature of these keratinocytes aligning a newly formed collagen IV, laminin V positive basement membrane within the hydrogel. In conclusion, we describe a RhS model containing neopapillae with hair follicle-inductive properties. Importantly, epidermal invagination occurred to engulf the neopapillae, thus demonstrating in vitro the first steps towards hair follicle morphogenesis in RhS.

KEYWORDS

epidermis, hair follicle, in vitro, neopapillae, reconstructed human skin, regenerative medicine

1 | INTRODUCTION

One of the major appendages traversing the skin is the hair follicle. The hair follicle plays a critical role in thermal regulation, dispersion of sweat and sebum, sensory and tactile functions, skin regeneration, and repigmentation (Paus & Cotsarelis, 1999; Stenn & Paus, 2001). Importantly, it also functions as a complex barrier between the environment and the circulatory system, the latter of which connects to the internal organs. The skin is continuously exposed to drugs, cosmetics, hair dyes, perfumes, household products, and industrial and agricultural products. The major penetration routes for substances coming into contact with the skin are via the outermost cornified layer (stratum corneum) and the hair shaft. Therefore, human skin models that closely represent hair biology are of major interest for basic research, in vitro drug testing and modelling skin disease such as alopeacia (hair loss). Furthermore, bioengineered human skin has emerged as a highly promising approach in regenerative medicine. However, autologous human skin constructs, currently used for the treatment of patients with full thickness wounds, are aimed at wound closure but do not restore hair growth (Blok et al., 2013; Gardien et al., 2016). The inability of the hair follicle to self-regenerate in current skin constructs may strongly impair posttransplantation quality of life in patients (Boyce & Lalley, 2018). In order to overcome this obstacle, autologous skin constructs are needed, that also include bioengineered human hair follicles.

Hair follicle development is induced and conducted by mesenchymal-epithelial cross-talk (Botchkarev & Kishimoto, 2003). Key regulators involved in the process are specialized fibroblast and keratinocyte-derived molecules of the Wnt, Hedgehog (SHH), and BMP (bone morphogenetic protein) signalling pathways, which are inhibited and activated in an alternating or combined manner. The dynamic interplay between these pathways generates different biomolecular gradients and thereby, a morphogenetic field that initiates the transitions between the different stages of hair follicle formation (Rishikaysh et al., 2014; Schmidt-Ullrich & Paus, 2005). While there is substantial knowledge on hair follicle biology, and a promising model to bioengineer single separated hair follicle equivalents already exists (Lindner, Horland, Wagner, Atac, & Lauster, 2011), most studies describe animal studies, mainly using mice. These studies aim at determining in detail how epidermal cell fate and dermal papillae cell heterogeneity are integrated in time and space to generate hair follicles (Adam et al., 2018; Schneider, Schmidt-Ullrich, & Paus, 2009). Complex mouse skin organoids constructed from pluripotent stem cells have been shown to develop de novo hair follicles resembling embryonic hair folliculogenesis (Lee et al., 2018). However, while being extremely informative, it can be expected that many findings reported from such animal studies cannot be directly extrapolated to the human situation due to important differences in skin biology and hair follicle cycling. For example, mice show hair follicle growth in cycles with a dormant catagen phase, activated telogen phase and fibre producing anagen phase (Muller-Rover et al., 2001; Stenn & Paus, 2001).

In contrast, human hair follicles are described to exist in two steady states called the active anagen (lasting years) and dormant telogen (lasting months) phases, which are separated by the transition phases catagen (regression) and neogen (regeneration; Al-Nuaimi, Goodfellow, Paus, & Baier, 2012; Bernard, 2012; Halloy, Bernard, Loussouarn, & Goldbeter, 2000). In order to create a more human-like model, human skin has been transplanted onto mice (Gilhar, Etzioni, & Krueger, 1990; Jahoda, Oliver, Reynolds, Forrester, & Horne, 1996). For example, adult human hair follicle neogenesis was observed when human neopapillae spheroids were first incorporated into human skin explants and then transplanted onto mice (Higgins, Chen, Cerise, Jahoda, & Christiano, 2013).

Previously, we have described a reconstructed human skin (RhS) model, which consists of a reconstructed epidermis grown on a dermal fibroblast-populated hydrogel, which is grown at the air–liquid interface (Kosten, Buskermolen, Spiekstra, de Gruijl, & Gibbs, 2015). Until now, the epidermis of RhS models constructed by us and others forms a flat, differentiated and stratified layer, which lacks the typical undulations, known as rete ridges (Buskermolen, Janus, Roffel, Krom, & Gibbs, 2018; el-Ghalbzouri, Gibbs, Lamme, Van Blitterswijk, & Ponec, 2002; Gibbs & Ponec, 2000). Our RhS model has been extensively characterized and compared with native skin biopsies. The epidermis has similar proliferation (Ki67 expression) and K10, K17, SKALP, involucrin, SPRR, and loricrin expression to native skin (Buskermolen et al., 2018; el-Ghalbzouri et al., 2002; Gibbs & Ponec, 2000). Crosstalk between the keratinocytes and fibroblasts results in the formation of a collagen IV and laminin containing basement membrane (el-Ghalbzouri et al., 2002). The model has been validated with respect to inflammatory cytokine release after chemical exposure and introduction of full thickness wounds (Breetveld, Richters, Rustemeyer, Scheper, & Gibbs, 2006; Buskermolen et al., 2016; Kosten, Buskermolen, et al., 2015). Further advancements have included introducing Langerhans Cells into the epidermis to investigate dendritic cell plasticity and migration in response to chemical stimuli and comparing the immune response to commensal and pathogenic oral biofilm (Buskermolen et al., 2018; Kosten, Spiekstra, de Gruijl, & Gibbs, 2015). In this current study, endothelial cells (ECs) were also included in the RhS as hair follicles are closely located to vascular structures (Hashimoto, Ito, & Suzuki, 1990; Montagna & Ellis, 1957). ECs were isolated and characterized as described previously and then seeded onto the lower side of the dermal matrix in order to mimic an in vivo endothelial barrier between RhS and the culture medium (Monsuur, van den Broek, Koolwijk, Niessen, & Gibbs, 2018). The aim of this study was to determine whether human neopapilla spheroids constructed from amplified dermal papillae cells, when incorporated into RhS, are able to maintain their inductive follicular properties when further cultured in vitro. Such a model, exclusively composed of primary human cells, would enable the investigation of human hair follicle biology in vitro.

2 | MATERIALS AND METHODS

2.1 | Human tissue and cell culture

Human juvenile foreskin was obtained after routine circumcisions from paediatric surgery. Occipital and temporal scalp skin follicular units, containing mainly growing anagen VI hair follicles, were obtained from disposed excess skin samples derived from adult male and female patients undergoing hair transplantation surgery. All skin samples were obtained in compliance with the relevant laws, with informed consent and ethical approval from the Ethics Committee of the Charite' Universitätsmedizin, Berlin, Germany, or with the "Code for Proper Secondary Use of Human Tissue" as formulated by the Dutch Federation of Medical Scientific Societies (www.federa.org) and approved by the institutional review board of the VU University medical centre.

Keratinocytes and fibroblasts were isolated from foreskin and cultured essentially as previously described (Kroeze et al., 2009; Kroeze et al., 2012). Keratinocytes were amplified in DermaLife medium (Lifeline Cell Technology, Carlsbad, CA) with added 1% penicillin/streptomycin (Corning, NY, USA) and switched to Keratinocyte medium-I during the week prior to constructing RhS. Keratinocyte medium-I contains Dulbecco's modified Eagle's medium (DMEM)/Ham's F12 (Corning) in a 3:1 ratio supplemented with 5% foetal clone III (Hyclone, UT, USA), 1 μmol/L hydrocortisone (Sigma-Aldrich, St. Louis, MO, USA), 1 μmol/L isoproterenol hydrochloride (Sigma-Aldrich), 0.1 μmol/L insulin (Sigma-Aldrich), 2 ng/ml human keratinocyte growth factor (Sigma-Aldrich), and 1% penicillin/streptomycin. Fibroblasts were cultured in DMEM with 5% foetal clone III and 1% penicillin/streptomycin.

Dermal papilla cells were isolated from human scalp tissue and cultured as previously described (Magerl, Kauser, Paus, & Tobin, 2002). In short, hairs were detached from small pieces of scalp under a binocular dissecting microscope using a scalpel and forceps. Next, the dermal papillae were isolated from the hair follicle and subsequently attached to the culture plate by a needle scratch. Multiple attached dermal papillae were cultured in follicle dermal papilla cell medium (Promocell, Heidelberg, Germany) and 1% penicillin/streptomycin. The dermal papilla cells migrated out of the dermal papilla within 4 weeks.

Foreskin dermal microvascular ECs were purified from the dermal cell fraction and cultured in Endothelial Cell Growth Medium MV2 (ECGM-MV2 medium; Promocell) and 1% penicillin/streptomycin as previously described (Schimek et al., 2013). In short, EC were purified using magnetic-associated cell sorting. After harvesting the cells with 0.05% Trypsin/EDTA (PPA, Coelbe, Germany), positive selection was preformed using CD31 MicroBead Kit (Miltenyi Biotec, Bergisch Gladbach, Germany) according to the manufacturer's instructions. After each magnetic-associated cell sorting purification step, a purity control was performed using FACS analyses until 90% of the cells were positive for CD31.

All cells were stored in the vapour phase of liquid nitrogen until required. For experiments keratinocyte passage 2, fibroblast passage 2 or 3, dermal papillae cells between passages 2 and 4, and ECs between passages 4 and 10 were used.

2.2 | Neopapillae construction

Neopapillae and fibroblast spheroids were constructed by seeding 3×10^4 cells/cm^2 into an ultra-low-attachment plate (Corning) in neopapillae-medium (DMEM containing 10% foetal bovine serum (Hyclone Laboratories Inc, Logan USA) and 1% penicillin/streptomycin) essentially as described previously (Lindner et al., 2011). Dermal papilla cells and fibroblasts were distributed well before placing in the incubator at 37°C, 5% CO_2, and 95% H_2O. Cells self-organized into condensates during a period of 6 days and were then further referred to as neopapillae and fibroblast spheroids. The dense spheroidal architecture of the spheroids was observed throughout the bulk cultures and repeatedly observed in independent repeats, confirming a reproducible neopapillae and fibroblast spheroid formation. Neopapillae medium was refreshed every 3 days, and neopapillae were introduced into RhS at day 6.

2.3 | Reconstructed human skin (RhS)

Dermal ECs were first seeded into a Millicell® insert of 9-mm inner diameter with 0.4-μm pore size (Merck, Darmstadt, Germany; 1.5×10^4 cells per insert) and cultured in ECGM-MV2 medium for 2 days. Next the fibroblast–neopapillae populated hydrogel was constructed: fibroblasts (7×10^4 cells/ml) were added to the collagen solution on ice (4 mg/ml collagen in 0.1% acetic acid isolated from rat tails). The fibroblast–hydrogel mixture (250 μl) was quickly pipetted into the Millicell® insert. After polymerization, a second collagen hydrogel (100 μl) containing fibroblasts (7×10^4 cells/ml) and neopapillae (approximately 90 neopapillae per gel) was pipetted on top of the first hydrogel. Hydrogels were cultured for 1 day submerged in Keratinocyte medium-I. Keratinocytes (6.5×10^4 cells/hydrogel) were then seeded on top of the hydrogel and cultured submerged for 3–4 days in Keratinocyte medium-I. Hereafter, RhS with neopapillae were further cultured at the air–liquid interface for another 10–14 days in Keratinocyte medium-II (DMEM/Ham's F12 (corning) in a 3:1 ratio supplemented with 1% foetal clone III, 1 μmol/L hydrocortisone, 1 μmol/L isoproterenol hydrochloride, 0.1 μmol/L insulin, 10 μmol/L L-carnitine (Sigma-Aldrich), 0.01 mol/L L-serine (Sigma-Aldrich), 50 μg/ml ascorbic acid (Sigma-Aldrich), and 1% penicillin/streptomycin. Control cultures were grown without the addition of neopapillae spheroids.

2.4 | Histology, immunohistochemistry, and immunofluorescent staining

Paraffin embedded sections (5 μm) were used for morphological (haematoxylin and eosin staining) and immunohistochemical analysis

of CD31 (clone JC70A, Dako, Glostrup, Denmark) as previously described (Monsuur et al., 2018). Frozen cryostat tissue sections (8 μm) were used for immunofluorescence staining with antibodies against chondroitin sulfate (clone CS-56, Abcam, Cambridge, UK), collagen IV (clone COL-95; Sigma Aldrich), cytokeratin 10 (clone VIK-10, ThermoFisher scientific, Waltham, USA), cytokeratin 15 (clone EPR1614Y, Abcam), fibronectin (clone FN-3, eBioscience San Diego, USA), laminin V (clone P3H9–2, R&D, Minneapolis, USA), or vimentin (clone EPR3776, Alexa Fluor® 594, Abcam) as previously described (Atac et al., 2013). A Keyence BZ-9000 Microscope with the BZ-II-Viewer software was used for microscopic imaging, and the images were merged using the BZ-II-Analyser software (Keyence, NeuIsenburg, Germany). Tissue sections were photographed using a Nikon Eclipse 80i microscope (Düsseldorf, Germany) with NIS elements AR 3.2 software (Nikon, Tokyo, Japan).

2.4.1 | Size measurement of neopapillae and dermal papillae

Photographs of the neopapillae bulk cultures at day 6 were taken using a phase contrast microscope. Three representative photos of each individual experiment were analyzed using NIS-elements AR software 3.2. Per experiment the width of 400 neopapillae was determined by measuring each neopapilla horizontally avoiding selection bias. As a reference the size of native dermal papillae was measured using heamatoxylin and eosin stained sections of a human scalp tissue.

2.5 | Neopapillae and fibroblast quantitative polymerase chain reaction

Human dermal skin fibroblasts (subconfluent monolayer), dermal papillae cells (subconfluent monolayer), 6-day-old neopapillae spheroids, and 6-day-old dermal fibroblast spheroids, cutured in neopapillea medium, were collected and snap frozen in liquid nitrogen and stored at −80°C. RNA isolation was carried out using the RNeasy Mini kit with on-column DNAse digestion (Qiagen, Hilden, Germany) according to the manufacturer's instructions. The production of cDNA and real-time polymerase chain reactions were carried out as previously described (van der Meijden et al., 2014), using RT2 First Strand Kit (Qiagen) and Fast SYBR Green Master Mix (Applied Biosystems, CA, USA) and quantitative polymerase chain reaction primer pairs (OriGene) for alkaline phosphatase (ALPL; HP200450), lymphoid enhancer-binding factor 1 (LEF1; HP212087), bone morphogenetic protein 4 (BMP4; HP205132), WNT5A (HP206917), WNT10B (HP206919), PDGFA (HP206262), vascular endothelial growth factor A (HP202779), and fibroblast growth factor 2 (FGF2; HP205762). Gene expression ($2^{-\Delta\Delta Ct}$) relative to that of dermal fibroblasts grown in monolayer or spheroid was normalized for the expression of housekeeping gene TATA box binding protein TBP (HP206762).

2.6 | Enzyme-linked immunosorbent assay

Culture supernatants from monolayer and spheroid cultures (see above) were collected and stored at −20°C for further analysis. For chemokine quantification in culture supernatants enzyme-linked immunosorbent assay (ELISA) reagents were used in accordance to the manufacturer's specifications. CCL2, CCL20, CXCL1, CXCL10, and IL-6 were measured by commercially available paired ELISA antibodies and recombinant proteins obtained from R&D System Inc. (Minneapolis, Minnesota). For CXCL8/IL-8 a Pelipair reagent set (CLB, Amsterdam, The Netherlands) was used. For CCL14a, CCL22, CCL24 and CXCL12, a DuoSet (R&D System Inc. Minneapolis, Minnesota) was used.

2.7 | Statistical analysis

Each experiment represents cells from a different donor with an intraexperiment duplicate. Three independent experiments were performed. Data are presented as mean, standard deviation, or standard error of the mean (SEM) as indicated. The differences between groups were tested for statistical significance using an unpaired T test or a Mann–Whitney test. Differences were considered significant when * $P < 0.05$. Statistics were calculated using GraphPad Prism 8 (San Diego, California, USA).
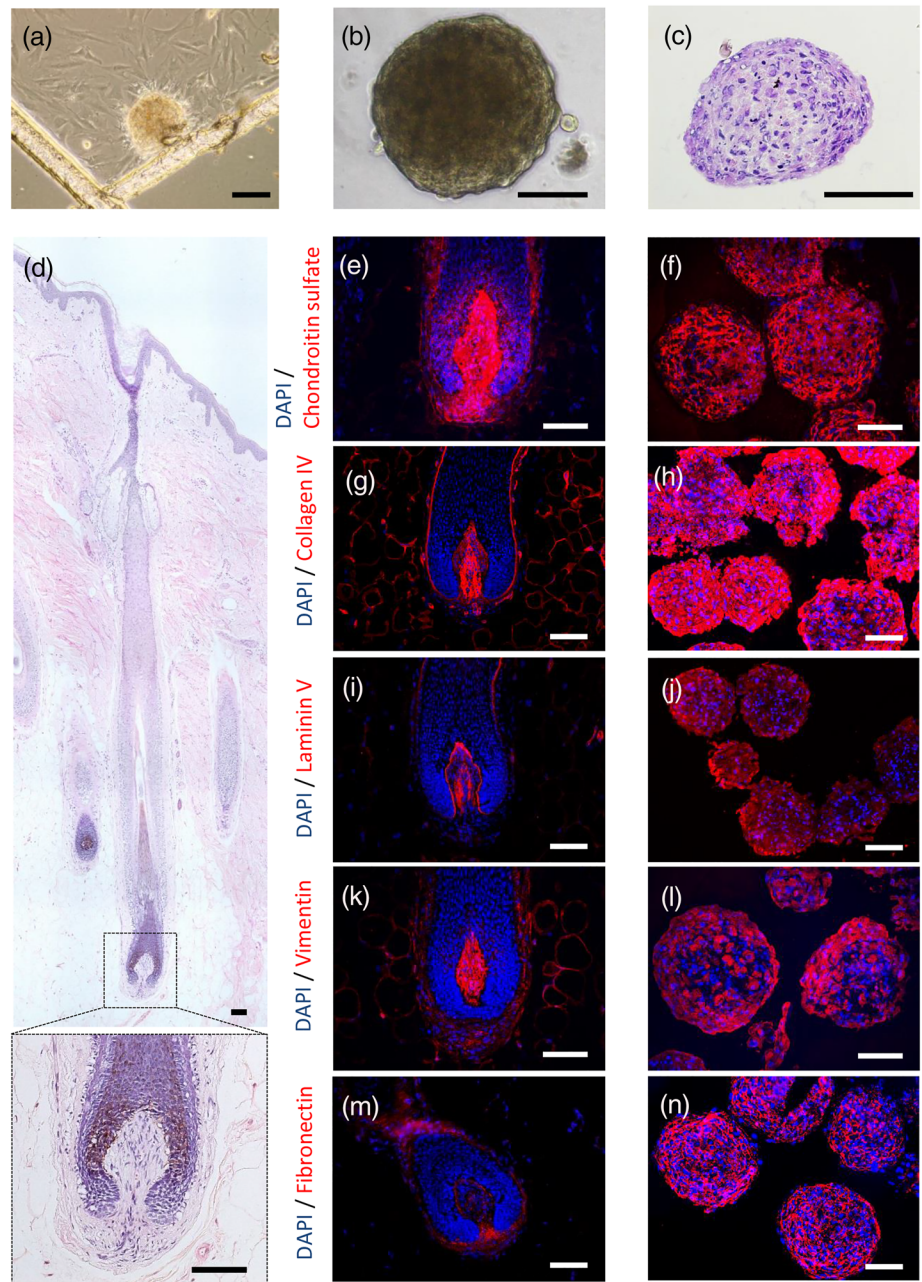
3 | RESULTS

3.1 | Comparison of cultured neopapillae spheroids with scalp hair dermal papillae

Dermal papillae consist of a dense sphere of cells and extracellular matrix (Figure 1). In order to determine in how far the in vitro grown neopapillae, which are reconstructed from amplified dermal papillae cells (Figure 1a–c), represent their native counterparts, an extensive characterization was performed. Native, dermal papillae (vimentin positive) located in the base of scalp hair follicle tissue expressed the extracellular matrix proteins chondroitin sulfate, collagen IV, laminin V, and fibronectin (Figure 1d,e,g,i,k,m). Notably, each of the 3D reconstructed neopapillae spheroids within the batch cultures also expressed these same extracellular matrix proteins (Figure 1f,h,j,l,n). Dermal papillae cells (DAPI staining) were observed evenly distributed throughout the extracellular matrix within the in vitro grown spheroids (Figure 1f,h,j,l,n). The diameter of the self-organized neopapillae spheroids ranged between 30 and 255 μm with the mean diameter of 111 μm (SEM ±13 μm). This diameter was comparable to that of dermal papillae found in scalp hair, which had a mean diameter of 97 μm (SEM ±16.6 μm; Figure 2a,b).

We further quantified mRNA levels in neopapillae spheroids and compared with dermal fibroblast subconfluent monolayers, since neopapilla spheroids would be expected to express different mRNA

FIGURE 1 Histological and immunofluorescence comparison between human scalp skin containing hair follicle and reconstructed neopapillae spheroids. (a) Light microscopic image showing dermal papilla cells growing out from an intact dermal papilla under submerged cell culture conditions. Self-assembly of dermal papilla cells into a neopapillae spheroid after 6 days of culture shown with (b) phase contrast image and (c) hematoxylin–eosin staining of tissue cryosection. (d) Hematoxylin–eosin staining of human scalp skin paraffin section containing hair follicle, showing the dermal papilla within the follicle bulb region. Immunofluorescence staining of (e, g, i, k, and m) human-hair follicle and (f, h, j, l, and n) neopapillae tissue sections with key markers for dermal papilla extracellular matrix: chondroitin sulfate (e and f), collagen IV (g and h), laminin V (I and j), vimentin (k and l), and fibronectin (m and n). DAPI shows cell nuclei. Scale bar = 100 μm [Colour figure can be viewed at wileyonlinelibrary.com]

transcripts that are relevant for hair formation compared with dermal fibroblasts, which are interspersed throughout the dermis as single cells (nonspheroid). Our results show that neopapillae, when compared with dermal fibroblasts, expressed more mRNA for multiple transcripts involved in rodent hair follicle neogenesis (Rishikaysh et al., 2014; Schmidt-Ullrich & Paus, 2005) and which are importantly found in human dermal papillae (Abaci et al., 2018; Higgins et al., 2013; Figure 2c). Neopapillae clearly expressed transcripts involved in initiating hair follicle formation: Wnt signalling pathway (WNT5a and WNT10b), LEF1, BMP4, platelet-derived growth factor (PDGF), vascular endothelial growth factor A, and ALPL. In contrast, transcript levels for FGF2 were downregulated. In order to determine

whether this differential gene expression was specific for dermal papillae cells within neopapillae and not an effect due to spheroid culture, gene expressions in monolayer cultures of dermal papillae cells and fibroblasts were compared. All genes were clearly upregulated in dermal papillae cells compared with fibroblasts again indicating that the dermal papillae cells had maintained their distinct gene expression profile compared with fibroblasts in culture (Figure 2d). Finally, when neopapillae spheroids were compared with that of fibroblast spheroids, again, WNT5a, WNT10b, and LEF1 were highly upregulated in the cultured neopapillae spheroids when compared with their fibroblast spheroid counterpart, in line with the other comparisons (Figure 2e).
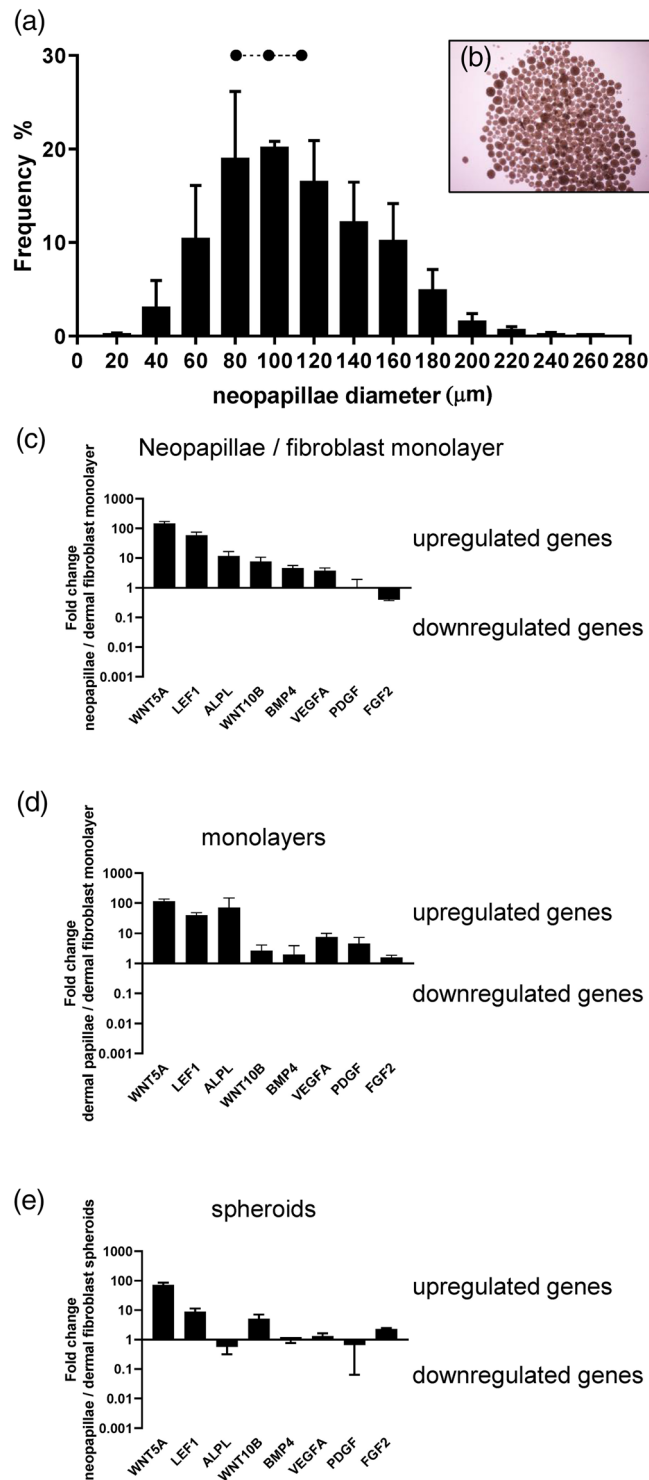
FIGURE 2 Neopapillae size and transcriptional characterization. (a) Distribution curve of neopapillae spheroid diameter (black bars) and scalp dermal papillae diameter (dashed line with circles). (b) Bulk culture showing 6-day-old neopapillae; (c) Quantification of mRNA transcript levels in neopapillae spheroids relative to dermal fibroblast subconfluent monolayers; (d) quantification of mRNA transcript levels in dermal papillae cells relative to fibroblasts both grown as subconfluent monolayers; (e) quantification of mRNA transcript levels in neopapillae spheroids relative to dermal fibroblast spheroids. Reverse transcription quantitative polymerase chain reaction. Fold change in gene expression was determined by normalizing levels to the housekeeping gene, TATA box binding protein TBP. All values represent a mean of at least three independent experiments with each experiment also representing a different donor; the arrow bars indicate standard deviation (*SD*) [Colour figure can be viewed at wileyonlinelibrary.com]
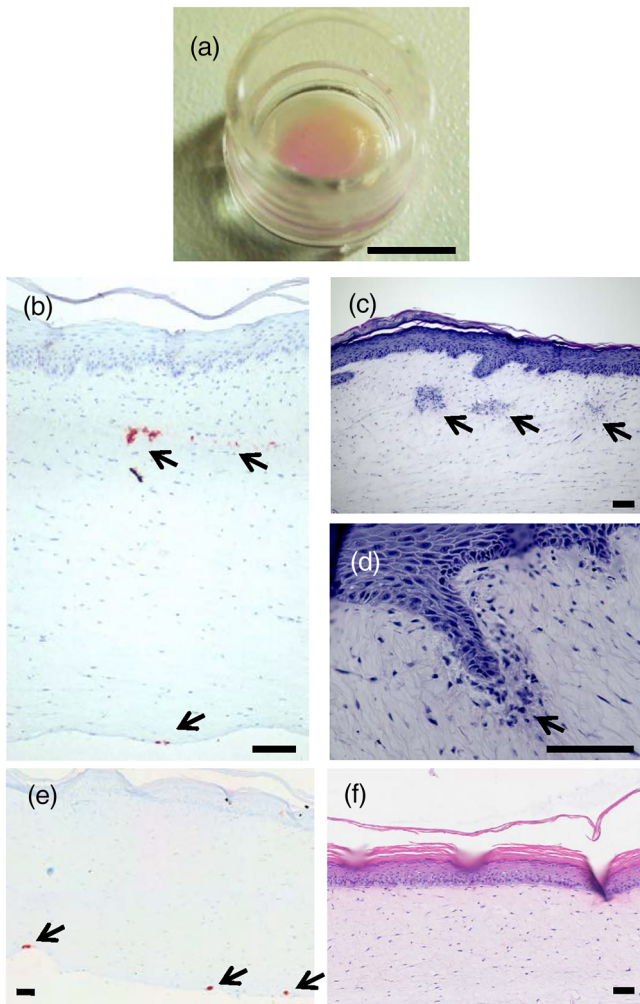
FIGURE 3 Reconstructed human skin (RhS) with integrated neopapillae spheroids after 10-day air-exposed culture (a–d). (a) Macroscopic view of skin equivalent culture; scale bar = 5 mm. (b) Immunohistological staining of CD31 showing endothelial cells located beneath and within the dermis of the RhS (red cells indicated by arrows). (c and d) Hematoxylin–eosin staining (paraffin section) of RhS showing invagination of epidermal keratinocytes in the vicinity of neopapillae (arrows show integrated neopapillae). (e and f) RhS without neopapillae spheroids. (e) Immunohistological staining of CD31 showing endothelial cells located beneath the RhS (red cells indicated by arrows). (f) Hematoxylin–eosin staining showing lack of epidermal invagination in absence of neopapillae. (b–f) Scale bar = 100 μm [Colour figure can be viewed at wileyonlinelibrary.com]

3.2 | RhS with incorporated neopapillae develop a hair-like inner and outer root sheath in vitro

Having determined that the neopapillae closely resembled their native dermal papillae counterparts by diameter, extracellular matrix composition, and gene expression, they were next incorporated into RhS (Figure 3). The RhS consists of a differentiated and stratified epidermis on top of the fibroblast populated hydrogel (Figure 3a). Single CD31 positive ECs where present within the hydrogel in close vicinity to the epidermis, indicating that they had migrated from the lower side of the hydrogel where they were seeded up towards the epidermal

keratinocytes (Figure 3b). No tubular EC structures were observed. Since only a few ECs, rather than the expected confluent layer, were observed on the lower side of the hydrogel, ECs were most probably lost during harvesting or tissue embedding in paraffin. Most strikingly, a downgrowth of the epidermis occurred in numerous places in the vicinity of the neopapillae within the hydrogel (Figure 3c,d). This downgrowth was not observed in RhS without neopapillae, even when ECs were present (Figure 3e,f), indicating that epidermal downgrowth was triggered by soluble mediators secreted from neopapillae, rather than ECs or fibroblasts. Furthermore, in the absence of neopapillae, ECs were only located on the lower side of the hydrogel where they had been seeded (Figure 3e).

In order to investigate this epidermal downgrowth in more detail, a phenotypic characterization of scalp skin was performed and compared with RhS with integrated neopapillae (Figure 4). Keratin 10 staining showed differentiated epidermal keratinocytes in human scalp, extending downwards to form the inner root sheath of the hair follicle with keratin 10 negative undifferentiated keratinocytes forming the outer root sheath (Figure 4a). The dense, round dermal papilla is found deep in the dermis and hypodermis of scalp and is strongly collagen IV positive together with the basement membrane aligning the hair shaft (Figure 4d). In line with this, RhS with neopapillae had a remarkably similar expression profile with keratin 10 differentiated keratinocytes invaginating the hydrogel to form an inner root sheath-like structure with undifferentiated keratin 10 negative keratinocytes on the outer side (Figure 4b,c). Collagen IV staining of serial sections with keratin 10 showed the neopapilla sphere located deep within the hydrogel and being completely engulfed by the invaginating epidermis (compare Figure 4b,c with Figure 4e,f). Similar to the native hair follicle, the outer side of the invaginating epidermis was keratin 15 positive confirming the undifferentiated nature of these keratinocytes aligning a newly formed collagen IV, laminin V positive basement membrane within the hydrogel (serial tissue sections; Figure 4g–i). Due to limitations in locating the neopapillae, the size of the neopapillae, and the thickness of the tissue sections, it was only possible to perform parallel stainings on maximally three consecutive tissue sections, and therefore, Figure 4b,c and Figure 4e,f show parallel staining emphasizing the engulfment of the neopapillae, and Figure 4g–i shows formation of the basement membrane and epidermal differentiation however sectioning missed the neopapillae.

3.3 | Neopapillae secrete higher amounts of keratinocyte chemoattractant cytokine CXCL1 than dermal fibroblasts

Since epidermal downgrowth into RhS only occurred when neopapillae were present, we next investigated which chemokines secreted by neopapillae spheroids might be responsible for this. Culture supernatants from the same monolayer and spheroid cultures, which were used to determine gene expression (Figure 2), were used to determine the presence of chemokines, which stimulate keratinocyte migration (Figure 5; Kroeze et al., 2009). Notably CXCL1
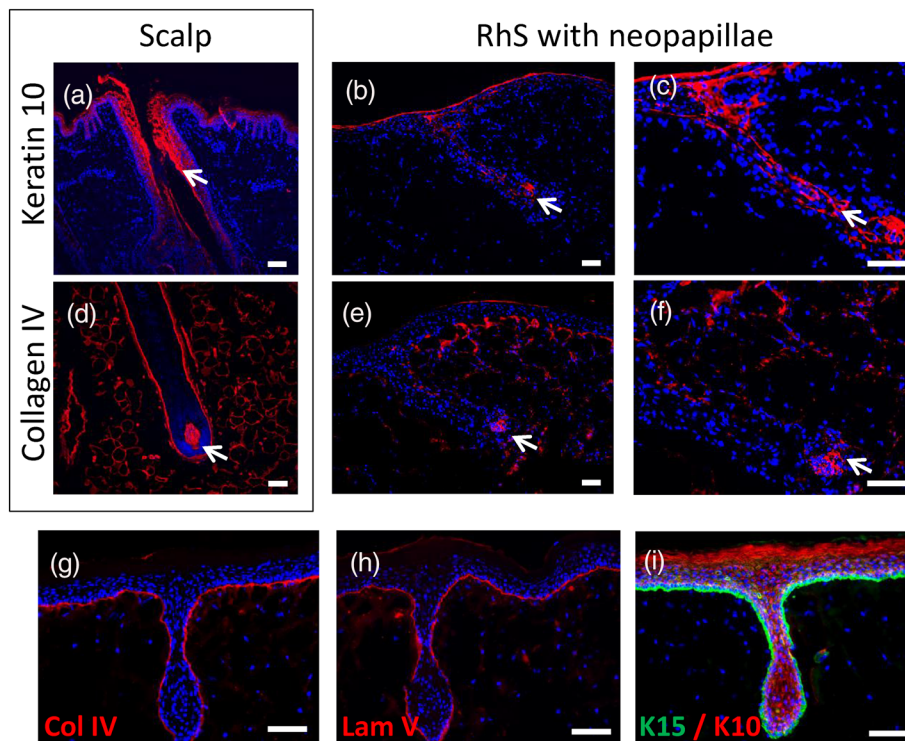
FIGURE 4 Immunofluorescence staining (cryosections) shows similarities between scalp skin and reconstructed human skin (RhS) containing neopapillae. (a) Keratin 10 (red) staining shows differentiated keratinocytes in scalp epidermis (infundibulum) and inner root sheath. (b and c) Keratin 10 staining in RhS epidermis and inner side of invaginating epidermis (red, arrows show invaginating differentiated keratinocytes). (d) Collagen IV (red) staining shows scalp hair follicle basement membrane and extracellular matrix of follicular dermal papillae. (e and f) Collagen IV staining of RhS basement membrane and extracellular matrix of neopapillae (red, arrow shows neopapillae). (b and e) Sequential RhS sections of the same tissue sample, with higher magnification shown in (c) and (f). (g) Collagen IV and (h) laminin V staining show basement membrane forming alongside invaginating epidermis; (i) keratin 10 (differentiated keratinocytes) and keratin 15 (basal layer keratinocytes) show inner and outer root sheath-like structures. (g–i) Sequential RhS sections of the same tissue sample. Cell nuclei were counterstained with DAPI (blue). Scale bar = 100 μm [Colour figure can be viewed at wileyonlinelibrary.com]

(significant) and CXCL8 (trend) amounts were higher in the dermal papillae cell cultures compared with fibroblast cultures (both monolayers and spheroids). In contrast, CXCL12 (monolayer and spheroid) and IL-6 (spheroid only) were lower in dermal papillae cell cultures. CCL14a, CCL20, CCL22, CCL24, and CXCL10 levels were below the detection limit (10–30 pg/ml) of the ELISA (data not shown).

Due to technical limitations, it was not possible to compare keratinocyte migration towards neopapillae and fibroblast conditioned culture media using our previously reported transwell chemotactic assay (Kroeze et al., 2009) since very high spontaneous migration was observed due to components already present in the culture media used to grow the neopapillae. Furthermore, when comparing keratinocyte migration towards unconditioned control media and cell conditioned media, less migration was observed in the cell containing condition, indicating that living cells had removed chemotactic molecules from the media rendering results nonconclusive (data not shown).

4 | DISCUSSION

Hair follicle morphogenesis is orchestrated by a complex morphogenetic mechanism throughout embryonic development. Although studies in rodent models during the last decades were particularly helpful to understand the dynamic molecular patterns of these events (Botchkarev & Kishimoto, 2003; Driskell, Clavel, Rendl, Watt, & Amagai, 2011; Rishikaysh et al., 2014; Schmidt-Ullrich & Paus, 2005; Schneider et al., 2009; St-Jacques et al., 1998), identification of signalling-pathways involved in human hair follicle morphogenesis remains a challenge. While there is abundant knowledge on hair follicle biology, as well as widespread interest in in vitro models for drug testing and clinical applications and also an easy accessibility of follicle cells, until now, it has proven to be extremely difficult to regenerate the human hair follicle within RhS in vitro. In this study, we show that neopapillae spheroids when incorporated into RhS undergo the first steps towards hair follicle morphogenesis. This indicates that even though the exact mechanisms are still difficult to decipher, the inductive phenotype of cultured human neopapillae spheroids is sufficient to result in epidermal invagination and engulfment of the neopapillae (see schematic diagram, Figure 6).

In 2013, Higgins et al. demonstrated that in vitro generated dermal papilla spheroids, composed of cultured human dermal papilla cells, were able to regain the transcriptional signature of the native follicular papilla. Remarkably, the spheroids were able to induce hair follicle neogenesis in a recipient foreskin when transplanted onto a back of a mouse (Higgins et al., 2013). In line with these findings, here we demonstrate that the three-dimensional architecture of condensed dermal papilla cells, already 6 days after initiating assembly, results in
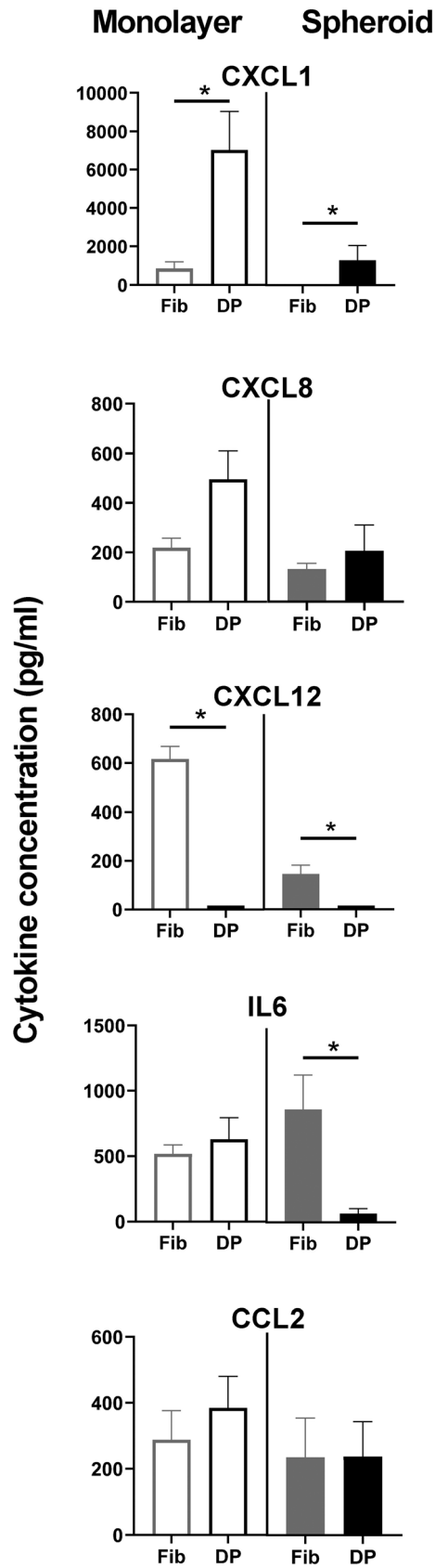
FIGURE 5 Chemokine production by dermal papillae cells and dermal fibroblasts. Culture supernatants from dermal papillae (DP) and fibroblast (Fib) monolayers and spheroid cultures were analysed for chemokine production by enzyme-linked immunosorbent assay. Each bar represents the mean ± standard error of the mean of three independent experiments each performed in duplicate. Statistical significant differences between Fib and DP were calculated using unpaired *T* test and Mann–Whitney test. Differences were considered significant when *P < 0.05
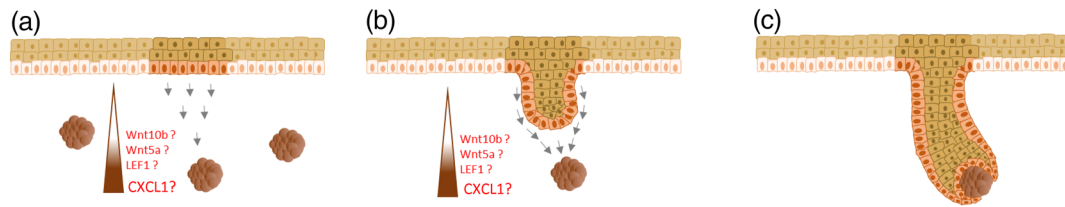
FIGURE 6 Schematic representation of reconstructed human skin showing epidermal invagination towards integrated neopapillae indicating early hair follicle formation in vitro. (a) Chemotactic gradient is generated in the dermis between the neopapilla spheroids and overlaying epidermal keratinocytes, (b) promoting the invagination of basal (orange) and differentiated keratinocytes (brown) towards the neopapilla. (c) Further epidermal downgrowth results in the engulfment of the neopapilla by the invaginating kerationcytes [Colour figure can be viewed at wileyonlinelibrary.com]

the expression of key signalling molecules and shows morphological characteristics of a native dermal papilla. Neopapillae naturally promoted the production of extracellular matrix environment characteristic of a follicular papilla. Moreover, when using 2D or spheroid cultured dermal fibroblasts (a typical nonfollicular mesenchymal cell within the dermis) for comparison, neopapillae spheroids showed a clearly different gene expression that may resemble newly condensed, follicular dermal papilla prior to maturation in human skin (Abaci et al., 2018; Higgins et al., 2013). It has been previously shown in human and mouse models that Wnt5a and Wnt10b signalling molecules are especially elevated in early stages of hair follicle morphogenesis and during the condensation and maturation of dermal papilla within the dermal condensate (Higgins et al., 2013; Reddy et al., 2001). Additionally, it has been suggested that LEF1 gene is one of the key factors that is required for epithelial-mesenchymal interaction during hair follicle morphogenesis (Abaci et al., 2018; DasGupta & Fuchs, 1999). Also, Higgins et al. presented a high expression of ALPL in newly formed dermal papilla and dermal sheath 6 weeks after spheroids where integrated within a foreskin recipient tissue (Higgins et al., 2013) and increased BMP4 may coincide with mature dermal papillae (Lin et al., 2015; Ohyama, Kobayashi, Sasaki, Shimizu, & Amagai, 2012). By growing dermal papillae cells in spheroids, we were able to maintain a similar expression of these key signalling molecules. In comparison to dermal fibroblasts, the RNA transcripts of Wnt5a, Wnt10b, LEF1, ALPL, and BMP4 molecules were upregulated in neopapillae spheroids, indicating their potential for human follicular inductivity. In contrast, at that given time point of neopapillae cultivation, FGF2 transcripts were downregulated and PDGF transcripts were the same. In many ways this finding is in line with rodent studies in which FGF-2 may inhibit the initiation and development of the mouse hair follicle (du Cros, 1993). PDGF may be more related to dermal development than specifically to hair follicle morphogenesis (Rezza, Sennett, Tanguy, Clavel, & Rendl, 2015). Taken together, our results might reflect the early stage of the dermal condensate prior to integration into RhS and before inducing molecular interactions with the overlaying epidermal cells and adjacent cells (fibroblasts and ECs) occur within the hydrogel since we clearly show that dermal papillae cells do maintain their distinct gene expression profile compared with fibroblasts in culture.

Studies in rodent models reported that hair-follicle morphogenesis is a gradient driven process, regulated by activating and inhibiting signalling molecule, such as Wnt, BMP, and FGF, secreted by mesenchymal condensing cells and the overlaying epithelial cells (Glover et al., 2017; Schmidt-Ullrich & Paus, 2005; Schneider et al., 2009). Recently, it has also been shown that the location of mesenchymal condensation during hair-follicle morphogenesis is initially dictated by the overlaying epidermis, generating local gradients of signalling molecules, such as FGF and TGFβ2 (Glover et al., 2017). These observations, together with our results, strongly suggest that the dense dermal papillae spheroid creates a strong chemotactic gradient to draw keratinocytes down into the hydrogel (Figure 6) and that similar mechanisms occur in humans as have previously been described for rodents. It is most probable that a multitude of chemotactic molecules being secreted from the dense neopapillae spheroid, rather than a single molecule, are working together in synergy and are responsible for the observed epidermal invagination. Our observation that large amounts of the keratinocyte chemoattractant cytokine CXCL1 (Kroeze et al., 2012) was secreted specifically from the dermal papillae cells compared with fibroblasts indicates that this molecule may be one of those involved in the invagination.

Previously, we have described that chemokine receptors on keratinocytes are involved in an autocrine feedback mechanism during reepithelialization after skin wounding in vitro (Kroeze et al., 2012). Furthermore, we have shown that fibroblasts are essential for maintaining epidermal integrity and that keratinocyte–fibroblast crosstalk is required for formation of the basement membrane (el-Ghalbzouri et al., 2002). Now, for the first time, we show that human dermal papillae also strongly influence keratinocyte behaviour to such an extent that they can induce the formation of a follicle like structure, which strongly reassembles the inner and outer root sheath of the hair appendage. In many aspects our results represent early stages of hair-follicle morphogenesis in which inductive reciprocal interaction between the epidermis and the underlying dermal condensate induces the organization of epidermal keratinocytes into a column that invaginates the dermis. It has yet to be determined whether extended culture will indeed enable a hair shaft to be grown in vitro. Also, notably, by introducing neopapillae into RhS, we observe for the first time structures similar to rete ridges, which have until now

always been absent in RhS models (Buskermolen et al., 2018; el-Ghalbzouri et al., 2002; Gibbs & Ponec, 2000), suggesting that the strong chemotactic gradient from neopapillae may be responsible. In support of our findings with human neopapillae, spherical skin organoids constituting epidermal and dermal layers, which are grown from a homogenous population of mouse-derived pluripotent stem cells, have been shown to spontaneously produce de novo hair follicles in a process that mimics normal mouse embryonic hair folliculogenesis in vitro (Lee et al., 2018). In line with Higgins et al. we show that neopapillae grown in spheroids have a papillae signature sufficient to initiate follicle morphogenesis (DasGupta & Fuchs, 1999; Reddy et al., 2001). Even though epithelial-mesenchymal interactions are clearly involved, the results obtained by us and Higgins et al. both showed hair follicle development in nonhair baring skin (foreskin) where there were no previous epidermal memory signals for hair follicle development present.

Abaci et al. (2018) has recently reported a ground breaking progress in the field of hair follicle engineering. For the first time they demonstrated hair follicle formation in skin equivalents when coseeding epidermal and dermal papilla cells into 3D imprinted microwells within a collagen hydrogel (dermis). The imprinted microwell was an essential factor since when dermal papilla spheroids were integrated into the skin equivalent, the spheroid dissociated within the dermis and failed to induce an epidermal-dermal interaction and invagination (Abaci et al., 2018). In contrast, in our study, we clearly observed for the first time invagination of the epidermis towards the neopapillae indicating epidermal-dermal interactions and potentially, self-assembling, de novo hair follicle formation already within the 10-day study period. Further experiments in the future will determine whether prolonged culture periods are sufficient to promote hair growth or whether additional paracrine signals from other cells are required.

Notably our study is an in vitro human study, which did not involve transplantation onto animals, and is therefore a significant advancement within the field of next-generation animal alternative methods with widespread implications for drug discovery as well as safety and efficacy testing of substances applied topically to the skin. Another potential application for skin models that contain viable neopapillae is in the field of advanced cell-based therapies. Whereas transplantation of intact follicular units (skin biopsies) is a proven successful technique for restoring hair loss (Avram, Finney, & Rogers, 2017), it still requires harvesting hair follicles from a donor site, and therefore, the technique is only suitable for small body areas and not for, for example, large (burn) wound areas. However, producing such a skin, which is fully compliant with the European regulations for advanced therapy medicinal products, would be a huge challenge.

In conclusion, we show that hair follicle formation can be initiated in vitro by incorporating neopapillae into air lifted RhS. It has yet to be determined whether extended RhS culture will indeed result in keratinized hair fibre growth or whether additional cell types are required within the model. We must however acknowledge the limitations of the current 2D microscopy techniques used in our study since we were unable to quantify the number of neopapillae and hair shafts within RhS since identifying their location was difficult nor could we investigate epidermal invagination at different time points. Such sampling at different time intervals would enable tracking of the invagination and EC migration into the hydrogel, as well as potential EC microcapillary formation to be studied. However, in order to do this in a way in which results can be quantified, a different imaging system, for example, 3D imaging, would be required since cells do not migrate along a perpendicular axis. This ambitious technical advancement is outside of the scope of the current study. However, already our model will provide a valuable tool to investigate human hair follicle formation in vitro without the use of animals as well as to test topically applied chemicals, which may penetrate the skin via the hair shaft. Moreover, our RhS with integrated neopapillae may be further developed in the future for transplantation on skin wounds in a one-step procedure. This will potentially allow hair follicle regeneration and hair growth in chronic wound and burns patients.

CONFLICT OF INTEREST

Uwe Marx and Gerd Lindner are cofounders of TissUse GmbH.

Gerd Lindner is the founder of the university spin off company provio GmbH.

Prof. Dr. R. J. Scheper and Prof. Dr. S. Gibbs were cofounders of A-SKIN Netherland BV, which was a VUmc skin tissue engineering spin off company (SME); this company ceased to exist in 2019.

The other authors have no conflicts of interest with regard to this manuscript.

AUTHOR CONTRIBUTIONS

All authors substantially contributed to design of experiments.

IV, MT, LvdB BA, SS, SG, and HM contributed to acquisition, analysis, and interpretation of data.

SG, IV, and MT drafted the manuscript.

All authors critically revised the manuscript and gave final approval.

ORCID

Susan Gibbs https://orcid.org/0000-0002-3446-6138

REFERENCES

Abaci, H. E., Coffman, A., Doucet, Y., Chen, J., Jackow, J., Wang, E., ... Christiano, A. M. (2018). Tissue engineering of human hair follicles using a biomimetic developmental approach. *Nature Communications*, 9(1), 5301. https://doi.org/10.1038/s41467-018-07579-y

Adam, R. C., Yang, H., Ge, Y., Lien, W. H., Wang, P., Zhao, Y., Polak, L., Levorse, J., Baksh, S. C., Zheng, D., & Fuchs, E. (2018). Temporal layering of signaling effectors drives chromatin remodeling during hair follicle stem cell lineage progression. *Cell Stem Cell*, 22(3), 398-413. e397. doi:https://doi.org/10.1016/j.stem.2017.12.004

Al-Nuaimi, Y., Goodfellow, M., Paus, R., & Baier, G. (2012). A prototypic mathematical model of the human hair cycle. *Journal of Theoretical Biology*, 310, 143–159. https://doi.org/10.1016/j.jtbi.2012.05.027

Atac, B., Wagner, I., Horland, R., Lauster, R., Marx, U., Tonevitsky, A. G., ... Lindner, G. (2013). Skin and hair on-a-chip: in vitro skin models versus ex vivo tissue maintenance with dynamic perfusion. *Lab on a Chip*, 13 (18), 3555–3561. https://doi.org/10.1039/c3lc50227a

Avram, M. R., Finney, R., & Rogers, N. (2017). Hair transplantation controversies. *Dermatologic Surgery*, 43(Suppl 2), S158–s162. https://doi.org/10.1097/dss.0000000000001316

Bernard, B. A. (2012). The human hair follicle, a bistable organ? *Experimental Dermatology*, 21(6), 401–403. https://doi.org/10.1111/j.1600-0625.2012.01457.x

Blok, C. S., Vink, L., de Boer, E. M., van Montfrans, C., van den Hoogenband, H. M., Mooij, M. C., ... Gibbs, S. (2013). Autologous skin substitute for hard-to-heal ulcers: retrospective analysis on safety, applicability, and efficacy in an outpatient and hospitalized setting. *Wound Repair and Regeneration*, 21(5), 667–676. https://doi.org/10.1111/wrr.12082

Botchkarev, V. A., & Kishimoto, J. (2003). Molecular control of epithelial–mesenchymal interactions during hair follicle cycling. *Journal of Investigative Dermatology Symposium Proceedings*, 8, 46–55. https://doi.org/10.1046/J.1523-1747.2003.12171.X

Boyce, S. T., & Lalley, A. L. (2018). Tissue engineering of skin and regenerative medicine for wound care. *Burns Trauma*, 6, 4. https://doi.org/10.1186/s41038-017-0103-y

Breetveld, M., Richters, C. D., Rustemeyer, T., Scheper, R. J., & Gibbs, S. (2006). Comparison of wound closure after burn and cold injury in human skin equivalents. *The Journal of Investigative Dermatology*, 126 (8), 1918–1921. https://doi.org/10.1038/sj.jid.5700330

Buskermolen, J. K., Janus, M. M., Roffel, S., Krom, B. P., & Gibbs, S. (2018). Saliva-derived commensal and pathogenic biofilms in a human gingiva model. *Journal of Dental Research*, 97(2), 201–208. https://doi.org/10.1177/0022034517729998

Buskermolen, J. K., Reijnders, C. M., Spiekstra, S. W., Steinberg, T., Kleverlaan, C. J., Feilzer, A. J., ... Gibbs, S. (2016). Development of a full-thickness human gingiva equivalent constructed from immortalized keratinocytes and fibroblasts. *Tissue Engineering. Part C, Methods*, 22(8), 781–791. https://doi.org/10.1089/ten.TEC.2016.0066

DasGupta, R., & Fuchs, E. (1999). Multiple roles for activated LEF/TCF transcription complexes during hair follicle development and differentiation. *Development (Cambridge, England)*, 126, 4557–4568.

Driskell, R. R., Clavel, C., Rendl, M., Watt, F. M., & Amagai, M. (2011). Hair follicle dermal papilla cells at a glance. *Journal of Cell Science*, 124, 1179–1182. https://doi.org/10.1242/jcs.082446

du Cros, D. L. (1993). Fibroblast growth factor and epidermal growth factor in hair development. *The Journal of Investigative Dermatology*, 101, 106S–113S. https://doi.org/10.1111/1523-1747.ep12363020

el-Ghalbzouri, A., Gibbs, S., Lamme, E., Van Blitterswijk, C. A., & Ponec, M. (2002). Effect of fibroblasts on epidermal regeneration. *The British Journal of Dermatology*, 147(2), 230–243.

Gardien, K. L., Marck, R. E., Bloemen, M. C., Waaijman, T., Gibbs, S., Ulrich, M. M., ... Dutch Outback Study, G. (2016). Outcome of burns treated with autologous cultured proliferating epidermal cells: A prospective randomized multicenter intrapatient comparative trial. *Cell Transplantation*, 25(3), 437–448. https://doi.org/10.3727/096368915X689569

Gibbs, S., & Ponec, M. (2000). Intrinsic regulation of differentiation markers in human epidermis, hard palate and buccal mucosa. *Archives of Oral Biology*, 45(2), 149–158. https://doi.org/10.1016/s0003-9969(99)00116-8

Gilhar, A., Etzioni, A., & Krueger, G. G. (1990). Hair growth in human split-thickness skin grafts transplanted onto nude rats: The role of cyclosporin. *Dermatologica*, 181(2), 117–121. https://doi.org/10.1159/000247898

Glover, J. D., Wells, K. L., Matthäus, F., Painter, K. J., Ho, W., Riddell, J., ... Headon, D. J. (2017). Hierarchical patterning modes orchestrate hair follicle morphogenesis. *PLoS Biology*, 15, e2002117. https://doi.org/10.1371/journal.pbio.2002117

Halloy, J., Bernard, B. A., Loussouarn, G., & Goldbeter, A. (2000). Modeling the dynamics of human hair cycles by a follicular automaton. *Proceedings of the National Academy of Sciences of the United States of America*, 97(15), 8328–8333. https://doi.org/10.1073/pnas.97.15.8328

Hashimoto, K., Ito, M., & Suzuki, Y. (1990). Innervation and vasculature of the hair follicle. In C. E. Orfanos, & R. Happle (Eds.), *Hair and hair diseases* (pp. 117–147). Berlin, Heidelberg: Springer Berlin Heidelberg.

Higgins, C. A., Chen, J. C., Cerise, J. E., Jahoda, C. A. B., & Christiano, A. M. (2013). Microenvironmental reprogramming by three-dimensional culture enables dermal papilla cells to induce de novo human hair-follicle growth. *Proceedings of the National Academy of Sciences of the United States of America*, 110, 19679–19688. https://doi.org/10.1073/pnas.1309970110

Jahoda, C. A. B., Oliver, R. F., Reynolds, A. J., Forrester, J. C., & Horne, K. A. (1996). Human hair follicle regeneration following amputation and grafting into the nude mouse. *Journal of Investigative Dermatology*, 107(6), 804–807.

Kosten, I. J., Buskermolen, J. K., Spiekstra, S. W., de Gruijl, T. D., & Gibbs, S. (2015). Gingiva equivalents secrete negligible amounts of key chemokines involved in Langerhans cell migration compared to skin equivalents. *Journal of Immunology Research*, 2015, 627125. https://doi.org/10.1155/2015/627125

Kosten, I. J., Spiekstra, S. W., de Gruijl, T. D., & Gibbs, S. (2015). MUTZ-3 derived Langerhans cells in human skin equivalents show differential migration and phenotypic plasticity after allergen or irritant exposure. *Toxicology and Applied Pharmacology*, 287(1), 35–42. https://doi.org/10.1016/j.taap.2015.05.017

Kroeze, K. L., Boink, M. A., Sampat-Sardjoepersad, S. C., Waaijman, T., Scheper, R. J., & Gibbs, S. (2012). Autocrine regulation of re-epithelialization after wounding by chemokine receptors CCR1, CCR10, CXCR1, CXCR2, and CXCR3. *The Journal of Investigative Dermatology*, 132(1), 216–225. https://doi.org/10.1038/jid.2011.245

Kroeze, K. L., Jurgens, W. J., Doulabi, B. Z., van Milligen, F. J., Scheper, R. J., & Gibbs, S. (2009). Chemokine-mediated migration of skin-derived stem cells: Predominant role for CCL5/RANTES. *The Journal of Investigative Dermatology*, 129(6), 1569–1581. https://doi.org/10.1038/jid.2008.405

Lee, J., Böscke, R., Tang, P. C., Hartman, B. H., Heller, S., & Koehler, K. R. (2018). Hair follicle development in mouse pluripotent stem cell-derived skin organoids. *Cell Reports*, 22(1), 242–254. https://doi.org/10.1016/j.celrep.2017.12.007

Lin, W.-H., Xiang, L.-J., Shi, H.-X., Zhang, J., Jiang, L. P., Cai, P. T., ... Xiao, J. (2015). Fibroblast growth factors stimulate hair growth through β -catenin and Shh expression in C57BL/6 mice. *BioMed Research International*, 2015, 1–9. https://doi.org/10.1155/2015/730139

Lindner, G., Horland, R., Wagner, I., Atac, B., & Lauster, R. (2011). De novo formation and ultra-structural characterization of a fiber-producing human hair follicle equivalent in vitro. *Journal of Biotechnology*, 152(3), 108–112. https://doi.org/10.1016/j.jbiotec.2011.01.019

Magerl, M., Kauser, S., Paus, R., & Tobin, D. J. (2002). Simple and rapid method to isolate and culture follicular papillae from human scalp hair follicles. *Experimental Dermatology*, 11(4), 381–385. https://doi.org/10.1034/j.1600-0625.2002.110414.x

Monsuur, H. N., van den Broek, L. J., Koolwijk, P., Niessen, F. B., & Gibbs, S. (2018). Endothelial cells enhance adipose mesenchymal stromal cell-mediated matrix contraction via ALK receptors and reduced follistatin: Potential role of endothelial cells in skin fibrosis. *Journal of Cellular Physiology*, *233*, 6714–6722. https://doi.org/10.1002/jcp.26494

Montagna, W., & Ellis, R. A. (1957). Histology and cytochemistry of human skin. XIII. The blood supply of the hair follicle2. *JNCI: Journal of the National Cancer Institute*, *19*, 451–463. https://doi.org/10.1093/jnci/19.3.451

Muller-Rover, S., Handjiski, B., van der Veen, C., Eichmuller, S., Foitzik, K., McKay, I. A., … Paus, R. (2001). A comprehensive guide for the accurate classification of murine hair follicles in distinct hair cycle stages. *The Journal of Investigative Dermatology*, *117*(1), 3–15. https://doi.org/10.1046/j.0022-202x.2001.01377.x

Ohyama, M., Kobayashi, T., Sasaki, T., Shimizu, A., & Amagai, M. (2012). Restoration of the intrinsic properties of human dermal papilla in vitro. *Journal of Cell Science*, *125*, 4114–4125. https://doi.org/10.1242/jcs.105700

Paus, R., & Cotsarelis, G. (1999). The biology of hair follicles. *The New England Journal of Medicine*, *341*(7), 491–497. https://doi.org/10.1056/NEJM199908123410706

Reddy, S., Andl, T., Bagasra, A., Lu, M. M., Epstein, D. J., Morrisey, E. E., & Millar, S. E. (2001). Characterization of Wnt gene expression in developing and postnatal hair follicles and identification of Wnt5a as a target of Sonic hedgehog in hair follicle morphogenesis. *Mechanisms of Development*, *107*, 69–82. https://doi.org/10.1016/S0925-4773(01)00452-X

Rezza, A., Sennett, R., Tanguy, M., Clavel, C., & Rendl, M. (2015). PDGF signalling in the dermis and in dermal condensates is dispensable for hair follicle induction and formation. *Experimental Dermatology*, *24*, 468–470. https://doi.org/10.1111/exd.12672

Rishikaysh, P., Dev, K., Diaz, D., Qureshi, W. M. S., Filip, S., & Mokry, J. (2014). Signaling involved in hair follicle morphogenesis and development. *International Journal of Molecular Sciences*, *15*, 1647–1670. https://doi.org/10.3390/ijms15011647

Schimek, K., Busek, M., Brincker, S., Groth, B., Hoffmann, S., Lauster, R., … Horland, R. (2013). Integrating biological vasculature into a multi-organ-chip microsystem. *Lab on a Chip*, *13*(18), 3588–3598. https://doi.org/10.1039/c3lc50217a

Schmidt-Ullrich, R., & Paus, R. (2005). Molecular principles of hair follicle induction and morphogenesis. *BioEssays*, *27*, 247–261. https://doi.org/10.1002/bies.20184

Schneider, M. R., Schmidt-Ullrich, R., & Paus, R. (2009). The hair follicle as a dynamic miniorgan. *Current Biology*, *19*(3), R132–R142. https://doi.org/10.1016/j.cub.2008.12.005

Stenn, K. S., & Paus, R. (2001). Controls of hair follicle cycling. *Physiological Reviews*, *81*(1), 449–494. https://doi.org/10.1152/physrev.2001.81.1.449

St-Jacques, B., Dassule, H. R., Karavanova, I., Botchkarev, V. A., Li, J., Danielian, P. S., … McMahon, A. P. (1998). Sonic hedgehog signaling is essential for hair development. *Current Biology*, *8*, 1058–1068. https://doi.org/10.1016/s0960-9822(98)70443-9

van der Meijden, K., Lips, P., van Driel, M., Heijboer, A. C., Schulten, E. A., den Heijer, M., & Bravenboer, N. (2014). Primary human osteoblasts in response to 25-hydroxyvitamin D3, 1,25-dihydroxyvitamin D3 and 24R,25-dihydroxyvitamin D3. *PLoS ONE*, *9*(10), e110283. https://doi.org/10.1371/journal.pone.0110283